THE JOURNAL OF BIOLOGICAL CHEMISTRY VOL. 281, NO. 8, pp. 4958–4968, February 24, 2006

ELOVL3 Is an Important Component for Early Onset of Lipid Recruitment in Brown Adipose Tissue*

Received for publication, October 26, 2005 Published, JBC Papers in Press, December 2, 2005, DOI 10.1074/jbc.M511588200

Rolf Westerberg[‡], Jan-Erik Månsson[§], Valeria Golozoubova[‡], Irina G. Shabalina[‡], Emma C. Backlund[‡], Petr Tvrdik[‡¶], Kjetil Retterstøl[‖], Mario R. Capecchi[¶], and Anders Jacobsson[‡1]

From the [‡]Wenner-Gren Institute, The Arrhenius Laboratories F3, Stockholm University, SE-106 91 Stockholm, Sweden, [§]Laboratory Medicine/Clinical Chemistry, Sahlgren's University Hospital, SE-431 80 Mölndal, Sweden, [¶]Howard Hughes Medical Institute, University of Utah, Salt Lake City, Utah 84112-5331, and [‖]Institute of Clinical Biochemistry, University of Oslo, Rikshospitalet, N-0027 Oslo, Norway

During the recruitment process of brown adipose tissue, the mRNA level of the fatty acyl chain elongase *Elovl3* is elevated more than 200-fold in cold-stressed mice. We have obtained *Elovl3*-ablated mice and report here that, although cold-acclimated *Elovl3*-ablated mice experienced an increased heat loss due to impaired skin barrier, they were unable to hyperrecruit their brown adipose tissue. Instead, they used muscle shivering in order to maintain body temperature. Lack of *Elovl3* resulted in a transient decrease in the capacity to elongate saturated fatty acyl-CoAs into very long chain fatty acids, concomitantly with the occurrence of reduced levels of arachidic acid (C20:0) and behenic acid (C22:0) in brown adipose tissue during the initial cold stress. This effect on very long chain fatty acid synthesis could be illustrated as a decrease in the condensation activity of the elongation enzyme. In addition, warm-acclimated *Elovl3*-ablated mice showed diminished ability to accumulate fat and reduced metabolic capacity within the brown fat cells. This points to ELOVL3 as an important regulator of endogenous synthesis of saturated very long chain fatty acids and triglyceride formation in brown adipose tissue during the early phase of the tissue recruitment.

Brown adipose tissue is the only tissue that functions exclusively to combust fat for heat production (1–3). When mammals encounter cold, there is an induced synthesis of specific mRNA species in brown adipose tissue, which encode enzymes regulating energy expenditure and lipid metabolism (4–6). Most notable is the increased mRNA level of the mitochondrial uncoupling protein 1 (UCP1), which can uncouple the mitochondrial respiratory chain and thereby dissipate heat instead of conserving energy in the form of ATP. The induction of processes needed for increased brown adipose tissue activity is referred to as brown fat recruitment.

The process is controlled by norepinephrine release from sympathetic nerve endings found in the tissue (7, 8) and can roughly be divided into two major phases, depending on how the animal experiences the cold (4 °C) (*i.e.* cold stress or cold acclimation). During the first days of cold exposure (*i.e.* cold stress), the major effect on brown adipose tissue is the initiation of hypertrophy, and a few days later, during the onset of cold acclimation, hyperplasia occurs (9, 10). After 4 days of cold exposure, there is a doubling in DNA amount, and after 3 weeks, a 3-fold increase is detected, which is the maximal level achieved with this degree of cold (11, 12). The increase in the total amount of protein in cold-exposed mice occurs also as a two-phase phenomenon (5). The first phase is completed within 3 days, and the second phase of protein increase (*i.e.* during cold acclimation) is found in the tissue after 2–3 weeks of cold exposure. During these events, protein synthesis mainly reflects an increase in mRNA levels (5).

During the process of identifying specific cDNA molecules corresponding to mRNA species that are induced in the brown adipose tissue upon cold stimulation (13), *Elovl3* (elongation of very long chain fatty acid) was identified. *Elovl3*, formerly denoted as *Cig30* (cold-induced glycoprotein of 30 kDa), is a member of a mammalian gene family whose products have been determined as being involved in the biosynthesis of very long chain fatty acids (VLCFAs)[2] (14, 15).

Except for brown adipose tissue, *Elovl3* mRNA was also detected in liver, skin, kidney, white adipose tissue, and heart, whereas no signal was detected in lung, testis, muscle, spleen, brain, thymus, and intestine (14, 15). Of particular interest is the fact that the expression of *Elovl3* was selectively elevated by more than 200-fold in brown adipose tissue of mice exposed to a 3-day cold stress. Prolonged cold exposure of mice for 1 month gradually decreased *Elovl3* expression, but the level still remained 100-fold above the control level. This phenomenon was qualitatively mimicked both by the continuous administration of norepinephrine via osmotic minipumps in mice kept at 28 °C and by intake of a calorie-rich diet (14). A similar increase in expression was detected during perinatal development, reaching a maximum level immediately after birth, demonstrating that *Elovl3* expression is highly correlated with recruitment of brown adipose tissue (14).

In recent years, the characterization of the ELOVL members has indicated that they are condensing enzymes and, as such, rate-limiting in the elongation machinery (16–20). Although the general function for the proteins is generally accepted, it is still not clear how the enzymes discriminate between different acyl chains as substrate (15, 20–23). ELOVL3 has, for example, been shown to elongate saturated and monounsaturated fatty acids up to 24 carbons. Both human and mouse models exist that either totally lack or have decreased levels of members of the ELOVL family (15, 19, 24, 25).

In order to ascribe a role to the ELOVL3 protein within brown adipose tissue during the recruitment process, we have obtained, by homologous recombination, a mouse strain that lacks a functional

* This work was supported by grants from the Swedish Research Council (to A. J. and J.-E. M) and by grants from the Howard Hughes Medical Institute and the Mathers Charitable Foundation (to M. R. C.). The costs of publication of this article were defrayed in part by the payment of page charges. This article must therefore be hereby marked "*advertisement*" in accordance with 18 U.S.C. Section 1734 solely to indicate this fact.

[1] To whom correspondence should be addressed: The Wenner-Gren Institute, The Arrhenius Laboratories F3, Stockholm University, Stockholm SE-106 91, Sweden. Tel.: 46-8-164127; Fax: 46-8-156756; E-mail: anders.jacobsson@wgi.su.se.

[2] The abbreviations used are: VLCFA, very long chain fatty acid; NE, norepinephrine; Tes, 2-{[2-hydroxy-1,1-bis(hydroxymethyl)ethyl]amino}ethanesulfonic acid; FCCP, carbonyl cyanide *p*-(trifluoromethoxy)phenylhydrazone; fluorescamine, 4-phenylspiro-[furan-2(3H), 1-phthalan]-3,3′-dione.

ELOVL3 protein. These mice exhibit a distinct skin phenotype, including impaired barrier function (25).

Surprisingly, although the *Elovl3*-ablated mice, compared with control mice, had a more than 100-fold reduced level of *Elovl3* mRNA in their brown adipose tissue when exposed to cold, a majority of the mice endured 4 °C cold exposure for several months. However, although the *Elovl3*-ablated mice experienced the cold more acutely, they were unable to hyperrecruit their brown adipose tissue. Instead, the *Elovl3*-ablated mice generated more heat by muscle shivering. As anticipated, the VLCFA elongation activity was significantly reduced in the brown adipose tissue of *Elovl3*-ablated mice exposed to the cold. Surprisingly, this phenomenon was only seen in mice during the initial cold stress. Cold-acclimated *Elov3*-ablated mice were equally efficient as normal mice at elongating fatty acids. In addition, warm-acclimated *Elovl3*-ablated mice showed dramatically reduced lipid accumulation within the brown adipocytes as well as reduced metabolic capacity when stimulated by norepinephrine. Since the difference in lipid formation between wild-type and *Elovl3*-ablated mice was transient (*i.e.* only seen in nonstimulated and acutely stimulated tissue), it implies that ELOVL3 is a critical enzyme for lipid accumulation and metabolic activity in brown adipocytes during the early phase of the tissue recruitment.

EXPERIMENTAL PROCEDURES

Animals—Elovl3-ablated mice were generated as described previously (25) and were back-crossed with C57Bl/6 (B & K Universal, Stockholm, Sweden). As control mice, age-matched mice from this backcross, which were bred under the same conditions as the *Elovl3*-ablated mice, were used. Where indicated, wild-type or heterozygote littermates from heterozygote *Elovl3*-ablated (+/−) intercrosses were used as control mice. During the course of the described experiments, no difference in results between the two control groups was noticed. Animals were fed *ad libitum* (Rat and Mouse Standard Diet No. 1; BeeKay Feeds; B & K Universal), had free access to water, and were kept in a 12 h/12 h light/dark cycle in single cages. Wild-type and Elovl3-ablated mice were bred at room temperature. Before the cold exposure experiments, the mice were kept at 30 °C (thermoneutrality) for 10 days where not indicated otherwise. After this period, animals were exposed to 4 °C for the indicated times or remained at 30 °C.

RNA Analysis—Total RNA was isolated using Ultraspec (Biotecx Laboratory) from 50–100 mg (w/w) of each tissue, as described earlier (14). For Northern blot analysis, total RNA was separated on a 1.2% (w/v) formaldehyde agarose gel and blotted onto Hybond-N membrane (Amersham Biosciences) in 20× SSC. The membrane was prehybridized with a solution containing 5× SSC, 5× Denhardt's solution, 0.5% SDS, 50 mM sodium phosphate, 50% formamide, and 100 mg/ml degraded DNA from herring sperm (Sigma) at 45 °C. After prehybridization, the membrane was transferred to a similar solution containing the denatured probe. The hybridization was carried out overnight at 45 °C. The membrane was then washed twice in 2× SSC, 0.2% SDS at 30 °C for 20–30 min each and then twice in 0.1× SSC, 0.2% SDS at 50 °C for 45 min. Corresponding cDNA fragments of Ucp1 (680 bp), Elovl1 (923 bp), and Elovl3 (980 bp) were used as probes as previously described (14, 15). The probes were labeled using a random-primed DNA labeling kit (Roche Applied Science) with [^{32}P]dCTP. The filters were analyzed on an Amersham Biosciences PhosphorImager and quantified with the ImageQuant program.

Reverse Transcription-PCR Transcription Analysis—DNase-treated total RNA (2.5 mg from interscapular brown fat) was reverse-transcribed using a Fermentas RevertAid^{TM} H Minus First Strand cDNA Synthesis Kit. The PCR reaction was carried out with *Taq* DNA polymerase (5 units/μl) and primers forward (exon 3) (5′-CGTAGTCAGATTCTGGTCCT-3′) and reverse (exon 4) (5′-CCAGAAGAAGTGTTCCGTTG-3′) for the *Elovl3* mRNA amplification, with the following cycle parameters: 94 °C for 2 min (1 cycle); 94 °C for 30 s, 64 °C for 30 s, 72 °C for 30 s (35 cycles); 72 °C for 2 min (1 cycle). The PCR products were electrophoresed in a 2% agarose gel in 0.5× TBE and photographed.

Body Temperature Measurement—Mice were housed at room temperature in single cages, and colonic temperature was measured (model BAT-12 thermometer; Physitemp Instruments Inc.) once before the experiment. The animals were then exposed to 4 °C for 8 h, during which colonic temperature was measured every 30 min.

In Vivo O_2 Consumption Measurement—Oxygen consumption measurements were performed in an open circuit system, as described by Dicker *et al.* (26). In all experiments, oxygen consumption was recalculated to ml of $O_2 \cdot min^{-1} \cdot (kg \text{ of body weight}^{-0.75})$. Before the experiment, the mice had been exposed to 30 °C or 4 °C for 3 weeks as indicated. Resting metabolic rate was measured at 30 °C for 3 h with the Somedic indirect calorimeter (50). The resting metabolic rate was defined as the mean of the three lowest 2-min oxygen consumption measuring points, during the last hour of the experimental period. A few days after the resting metabolic rate measurements, the thermogenic response to norepinephrine (NE) was measured. The animals were injected with sodium pentobarbital (pentobarbital natricum; 90 mg/kg of body weight intraperitoneally, final volume 0.3 ml; Apoteksbolaget, Stockholm, Sweden) and transferred to the calorimetric chamber at 30 °C. After about 30 min, when the metabolic rate during anesthesia had stabilized, NE (1 mg/kg of body weight, (−)-arterenol bitartrate; Sigma) was injected subcutaneously dissolved in physiological saline in a final volume of 0.1 ml. For measurements of metabolic rate at different environmental temperatures (thermoneutrality (30 °C), room temperature (21 °C), and acute response to mild (15 °C) and heavy (4 °C) cold stress), the animals were kept in the chamber at the relevant temperature for 1 h. The metabolic rate was determined as the mean rate of oxygen consumption within the last 20 min of the 1-h period.

Mitochondrial O_2 Consumption Measurement—Brown adipose tissue mitochondria were isolated and analyzed in parallel from male 10–14-week-old wild-type and *Elovl3*-ablated mice. Interscapular, periaortic, and axillary brown adipose tissue of four mice was pooled and used for isolation of mitochondria. The standard procedure of differential centrifugation was modified as described by Cannon and Nedergaard (27). Mitochondria were isolated using medium consisting of 250 mM sucrose that in final centrifugation was changed to medium containing 20 mM K^+-Tes (pH 7.2), 100 KCl, 0.6% fatty acid-free bovine serum albumin in order to re-expand the mitochondrial matrix. Mitochondrial protein concentration was measured using the 4-phenylspiro-[furan-2(3H),1-phthalan]-3,3′-dione (fluorescamine) method (28), and the suspensions were diluted to stock concentrations of 25 mg of mitochondrial protein/ml in 20 mM K^+-Tes (pH 7.2), 100 KCl with 0.3% fatty acid-free bovine serum albumin. Oxygen consumption rates were monitored with a Clark-type oxygen electrode (YSI Inc.) in a sealed chamber at 30 °C. The output signal from the oxygen electrode amplifier was electronically time-differentiated and collected every 0.5 s by a PowerLab/ADInstrument (application program Chart version 4.1.1). Mitochondria (0.3 mg of protein/ml) were incubated in medium consisting of 100 mM KCl, 20 mM K^+-Tes (pH 7.2), 2 mM $MgCl_2$, 1 mM EDTA, 4 mM KP_i, 3 mM malate, and 0.3% fatty acid-free bovine serum albumin.

Palmitoyl-CoA, carbonyl cyanide *p*-(trifluoromethoxy)phenylhydrazone (FCCP), oligomycin, GDP (sodium salt), L-(−)-malic acid (diso-

dium salt), pyruvic acid (sodium salt), and EDTA were all from Sigma. GDP was dissolved in 20 mM K^+-Tes (pH 7.2), and the solution was readjusted in pH. Fluorescamine was from Fluka. FCCP was dissolved in 50% ethanol; oligomycin was dissolved in 95% ethanol. Palmitate (sodium salt) and palmitoyl-L-carnitine were dissolved in 90% ethanol. Ethanol in a final concentration of 0.1% did not in itself have any effects on the parameters measured.

Preparations of Microsomes and the Fatty Acid Elongation Assay—Interscapular brown adipose tissue was dissected and homogenized in 4 ml of ice-cold 0.25 M sucrose. Following a 30-min stepwise centrifugation (10 min at 700 × *g*, 8,000 × *g*, and 17,000 × *g*) at 4–10 °C, the supernatant was carefully transferred to fresh tubes, and microsomes were sedimented at 105,000 × *g* for 45 min. The pellet was resuspended in 20 mM Tris-HCl (pH 7.4) containing 0.4 M KCl and centrifuged at 105,000 × *g* for 45 min. The final microsomal pellet was resuspended in 200 μl of 0.1 M Tris-HCl (pH 7.4), and the protein concentration was determined according to Bradford (29).

Total fatty acid elongation activity was measured essentially according to Suneja *et al.* (19). The assay mixtures (0.5 ml total, including a 25-μg protein addition) contained 0.1 M Tris-HCl (pH 7.4); either 50 μM palmitoyl-CoA (C16:0) or 15 μM arachidoyl-CoA (C20:0); substrate/bovine serum albumin ratio of 2:1; 1 mM NADPH; and 50 μM malonyl CoA (containing 0.050 μCi of [2-^{14}C]malonyl-CoA). The reaction was carried out for 17 min at 37 °C and terminated by the addition of 0.5 ml of 15% KOH in methanol and saponified at 65 °C for 45 min. The samples were cooled and acidified with 0.5 ml of cold 5 M HCl. Free fatty acids were extracted from the mixture three times with 1.5 ml of *n*-hexane and dried under vacuum. The extract was dissolved in 1 ml of chloroform and measured for radioactivity, after the addition of 10 ml of scintillation mixture, in a Beckman liquid scintillation system 3801.

The assay conditions for determining the condensation reaction were the same as for total elongation activity, except that NADPH was omitted from the mixture.

Lipid Analysis—Samples of about 100 mg of tissue were used for lipid extraction with 3 ml of chloroform/methanol/water 4:8:3 (by volume) (30). After centrifugation, the sediment was extracted with another portion of the same solvent. The combined supernatants were evaporated to dryness and dissolved in chloroform/methanol/water 60:30:4.5 (by volume). Low molecular weight contaminants and gangliosides were removed by partition against 0.1 M KCl in the proportion chloroform/methanol/KCl, 4:2:1. After centrifugation, the upper phase was removed and discarded. Lipid extract corresponding to 10 mg of tissue was evaporated to dryness under nitrogen. Heptadecenoic acid methyl ester was added as an internal calibrator. Transmethylation was performed with 0.2 M sodium methylate in methanol for 2 h at 60 °C. The fatty acid methyl esters formed from glycerolipids and cholesterol esters were purified from cholesterol and sphingolipids by thin layer chromatography with methylene chloride as developing solvent. The purified fatty acid methyl ester fraction was assayed by gas chromatography on a DB-23 column (30 m × 0.53 mm inner diameter, J&W Scientific, Folsom, CA). The total amount of fatty acids was calculated using the internal calibrator and expressed as μmol/g of fresh tissue, and the fatty acid compositions are given as molar distributions/mol %. The between-day coefficients of variation varied between 0.9 and 3.5% for the different fatty acids. Total fat content was measured in three or four anesthetized mice of each group using a DEXA scanner from Lunar/GE Medical Systems (PIXImus2). DEXA scans, except for head regions, were analyzed using the PIXImus2 software (version 1.46.007). The percentage of fat was obtained by dividing total fat content (g) by total tissue mass.

Electromyogram Measurements—Electromyogram recordings were obtained principally as in Ref. 31. Mice were anesthetized with halothane, and then safety pin-type electrodes (two recording, one reference) were placed over the back muscles of the mice. After recovery from anesthesia, the mice were placed in the chamber with a defined ambient temperature. Recording was started at 4 °C, and then the temperature in the chamber was increased to 30 °C, where basal muscle activity was measured.

The electromyogram signal picked up by the electrodes was amplified (×1,000) and noise-filtered (high pass filter 10 Hz, low pass filter 3 kHz) with a low noise preamplifier (World Precision Instruments) and rectified and integrated in a purpose-built RC integrator, principally as in Ref. 32. The signal from the RC integrator, corresponding to a running mean over 37.6 s, was digitalized and recorded with a MacLab system at a rate of 40 data points/min. The data obtained in this way represented the mean rectified value (U_{mrv}), as defined in Ref. 32, which is equivalent to the mean deviation around the sample mean. Electromyogram measurements in cold and at thermoneutrality were performed on the same experimental occasion.

Histology—Interscapular brown adipose tissue was taken from age- and sex-matched animals. Specimens were fixed in 10% buffered formaline for 24 h and embedded in paraffin. Sections were cut at 4 μm, stained with hematoxylin and eosin, and examined by light microscopy.

RESULTS

Normal Body Temperature in Elovl3-ablated Mice—We have shown previously that *Elovl3* gene expression is induced in brown adipose tissue in mice under circumstances when a high demand for heat production is required (14). The Northern blot in Fig. 1*A* shows the increase in *Elovl3* mRNA in mice exposed to the cold, reaching maximum levels between days 1 and 3. This corresponds to an approximately 100-fold increase in *Elovl3* mRNA, compared with the level in control mice housed at 30 °C. Prolonged exposure of the mice to 1 month of cold gradually decreased the *Elovl3* mRNA expression to about 60% of the maximum value. In the *Elovl3*-ablated mice, there was no detectable *Elovl3* mRNA species in cold-exposed (*i.e.* 3 days at 4 °C) or in cold-acclimated (*i.e.* 3 weeks at 4 °C) mice (Fig. 1*B*).

Compared with wild-type mice, *Elovl3*-ablated mice displayed a tousled hair coat. In addition, the mice exhibit a disturbed hair lipid content, resulting in a severe defect in water repulsion and increased transepidermal water loss (25). This has dramatic effects on the thermoregulation of the *Elovl3*-ablated mice, since wet fur led to a severe drop in body temperature within 1 h (25). To further investigate the ability of the *Elovl3*-ablated mice to control their body temperature, we acutely exposed the mice to cold (4 °C) and measured their colonic temperature during an 8-h period. Surprisingly, although there was a slight drop in body temperature during the first hours in cold, there was no significant difference between wild-type and *Elovl3*-ablated mice (Fig. 1*C*). However, with increased number of experiments and mice used, we could detect a sporadic mortality among *Elovl3*-ablated mice within the first 24 h of cold exposure. The majority of the *Elovl3*-ablated mice seemed, however, to be fully normal with respect to their ability to maintain body weight and body temperature even after several weeks of cold exposure (data not shown).

Hyperinduced Metabolic Rate in Cold-exposed Elovl3-ablated Mice—Since the *Elovl3*-ablated mice were capable of sustaining normal body temperature, we assumed that a normal heat-producing function of brown adipose tissue is maintained in the ablated mice. In order to confirm this, we measured oxygen consumption in cold-acclimated wild-type and *Elovl3*-ablated mice. As seen in Fig. 2*A*, no difference in

oxygen consumption between cold-acclimated wild-type and *Elovl3*-ablated mice could be detected at thermoneutral temperature (30 °C). As expected, there was a gradual increase in the demand for heat production in both mouse strains with decreased environmental temperature, but remarkably, the increase was constantly higher in *Elovl3*-ablated mice. The difference was most pronounced in mice kept at 4 °C, where the *Elovl3*-ablated mice showed a 40% higher increase than the control mice (Fig. 2*A*). This demonstrates that the *Elovl3*-ablated mice require more heat production for body temperature defense than the control mice upon cold exposure, presumably because of their poorer insulation (25), indicated by the greater slope of the oxygen consumption curve.

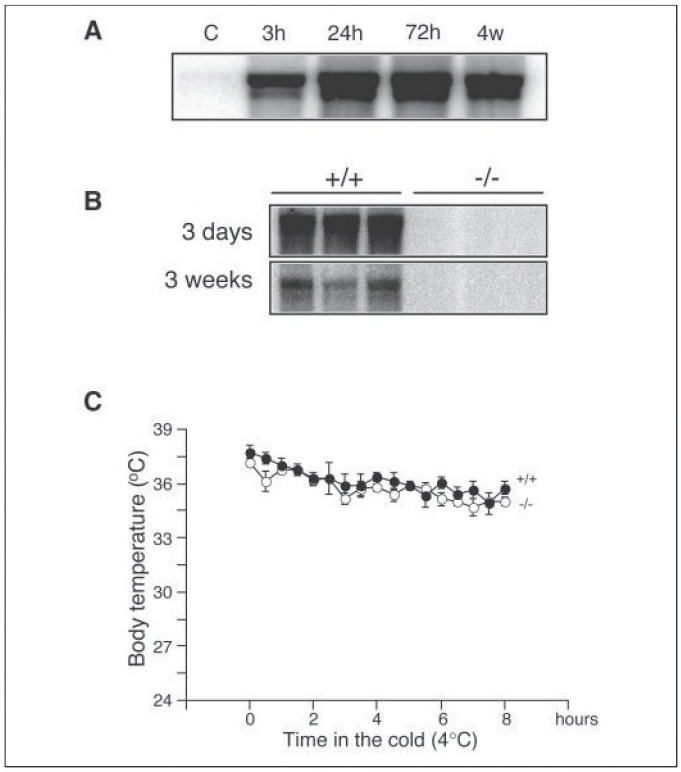

FIGURE 1. **RNA levels and body temperature in brown adipose tissue of *Elovl3*-ablated mice.** *A*, *Elovl3* mRNA levels in tissues taken from wild-type mice exposed to 30 °C (control) or 4 °C for 3 h, 24 h, 72 h, or 4 weeks, respectively. *B*, *Elovl3* mRNA levels in tissues taken from wild-type (+/+) and *Elovl3*-ablated mice (−/−) exposed to cold (4 °C) for 3 days or 3 weeks. Each group is represented by three animals. Ten μg of total RNA was loaded into each lane. *C*, mice were exposed to 4 °C for 8 h, and colon temperature was measured every 30 min. The values are expressed as mean ± S.E. of eight wild-type (*filled circles* and indicated by +/+) and eight *Elovl3*-ablated (*open circles* and indicated by −/−) animals, respectively, at each point.

Oxidative Capacity of Brown Adipose Tissue in Elovl3-ablated Mice—The observation that *Elovl3*-ablated mice showed a hyperinduced metabolic rate at 4 °C even after a prolonged time in cold indicated a higher capacity for brown fat-mediated nonshivering thermogenesis (*cf.* Golozoubova (31)). The nonshivering capacity can be determined by injection of norepinephrine, the mediator of heat production in brown adipose tissue.

Norepinephrine was injected, at thermoneutrality, into wild-type and *Elovl3*-ablated mice that had previously been acclimated to 4 °C. As expected, wild-type animals responded with a large increase in oxygen consumption (Fig. 2*B*), which was equal to the oxygen consumption observed in the cold. In the *Elovl3*-ablated mice, the effect of norepinephrine was identical to that in the wild-type mice (Fig. 2*B*), which is far below that required by the *Elovl3*-ablated mice at 4 °C (Fig. 2*A*). This demonstrates that the hyperinduced metabolic rate in *Elovl3*-ablated mice was not due to a greater capacity of BAT for heat production.

Normal Mitochondrial UCP1 Activity and Oxidative Capacity in Elovl3-ablated Mice—The heat production of the brown adipocyte is obtained through an uncoupling mechanism of the mitochondrial respiratory chain (33). The synthesis of the uncoupling protein 1 (UCP1) has been shown to be regulated by norepinephrine directly via its mRNA (5). In order to see if the suboptimal capacity of the brown adipose tissue, in the absence of *Elovl3*, could be explained by impaired *Ucp1* expression, we analyzed *Ucp1* mRNA levels in both cold-stressed and cold-acclimated *Elovl3*-ablated mice. Although there was a larger variation of *Ucp1* expression within the *Elovl3*-ablated mice after 3 days of cold exposure, as seen in Fig. 3*A*, there was no significant difference in *Ucp1* mRNA levels between *Elovl3*-ablated mice and control mice.

As elucidated from studies of UCP1-ablated mice, brown fat mitochondria from wild-type mice exhibit innate UCP1-dependent high oxygen consumption (uncoupling) that can be inhibited by GDP and reactivated by fatty acids (3, 34). To see whether this innate uncoupling was affected by the ELOVL3 deficiency, we analyzed mitochondria from *Elovl3*-ablated mice. As seen in Fig. 3*B* and Table 1, basal rates of oxygen consumption, in the presence of substrate (pyruvate), and UCP1-dependent oxygen consumption, calculated as difference between substrate-stimulated and GDP-inhibited oxygen consumption rates, were not different from brown fat mitochondria isolated from wild-type mice, indicating that UCP1 activity is independent of ELOVL3 activity. In addition, the oxidative capacity, estimated as maximal oxygen consumption induced by the uncoupler FCCP, was not different in brown fat mitochondria isolated from wild-type and *Elovl3*-ablated mice.

Mitochondrial fatty acid oxidation is the major source of energy for heat production in brown adipose tissue (6). To see if fatty acid activation, transport, or mitochondrial fatty acid combustion was affected by deletion of ELOVL3, experiments were designed to examine each of these steps.

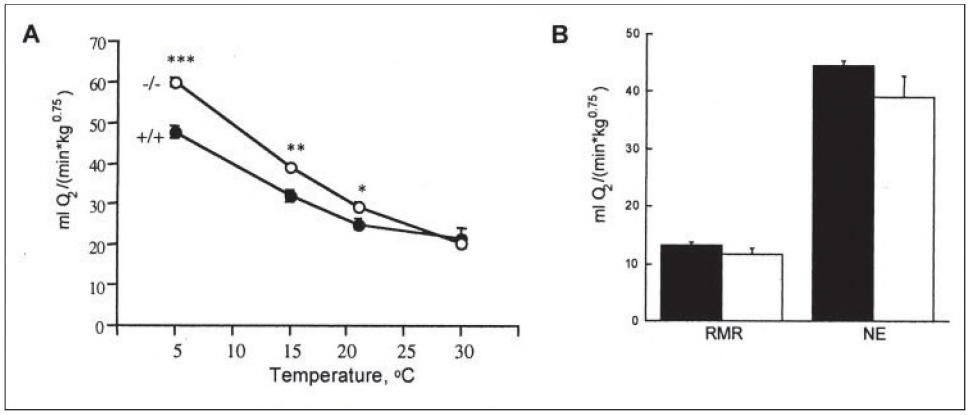

FIGURE 2. **Hyperinduced metabolic rate in *Elovl3*-ablated mice.** *A*, oxygen consumption of cold-acclimated mice for 1 h at different environmental temperatures. Each point represents five wild-type (+/+) and five *Elovl3*-ablated (−/−) animals with corresponding S.E. Statistical difference between wild-type (*filled circles*) and *Elovl3*-ablated mice (*open circles*) are calculated with an unpaired *t* test. *, $p < 0.05$; **, $p < 0.01$; ***, $p < 0.001$. *B*, resting metabolic rate (*RMR*) of 4-week cold-acclimated (4 °C) wild-type and *Elovl3*-ablated mice determined at thermoneutrality (30 °C) in a metabolic chamber at 30 °C for 3h. NE (1 mg/kg of body weight) was injected at 30 °C. The values represent means ± S.E., based on five wild-type mice (*black bars*) and five *Elovl3*-ablated mice (*open bars*) in each group.

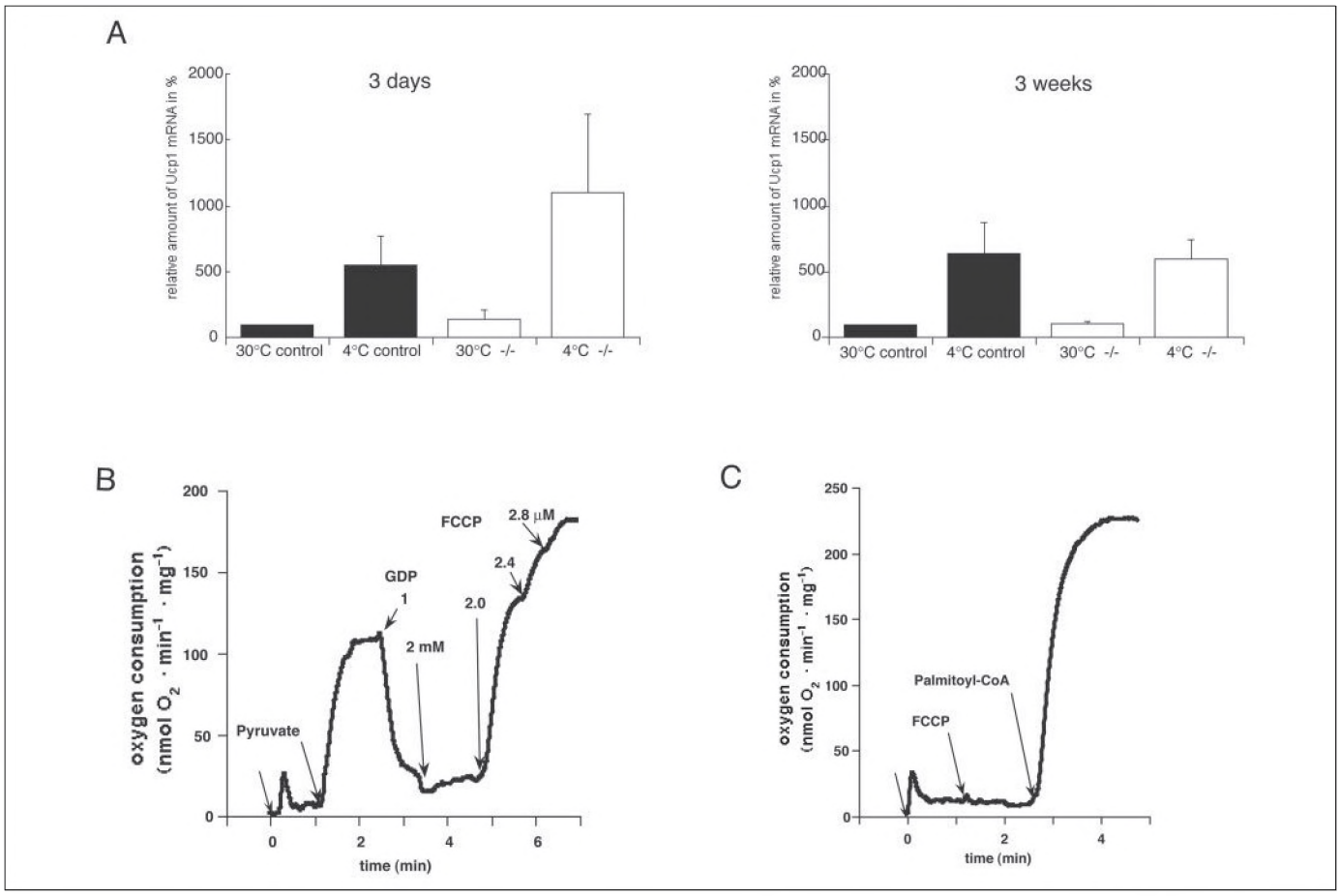

FIGURE 3. **Normal mitochondrial capacity in *Elovl3*-ablated mice.** *A*, *Ucp1* mRNA levels in brown adipose tissue taken from wild-type (+/+) and *Elovl3*-ablated mice (−/−) cold-exposed (4 °C) for 3 days (*left*) or 3 weeks (*right*). *Ucp1* mRNA levels from wild-type mice kept at 30 °C were set to 100%, and the values are expressed as mean ± S.E. from two independent experiments with three mice in each group. *B*, mitochondrial analysis of UCP1 activity. Representative trace showing the effects of GDP and FCCP on oxygen consumption supported by pyruvate in brown adipose tissue mitochondria isolated from *Elovl3*-ablated mice. The additions were 0.3 mg of brown fat mitochondria (*M*) and 5 mM pyruvate. GDP and FCCP were successively added to the indicated final concentrations. *C*, mitochondrial analysis of fatty acid oxidation. Representative trace showing a recording from oxygen consumption measurements of brown-fat mitochondria supported by palmitoyl-CoA in the presence of DL-carnitine. The additions were 0.3 mg of brown fat mitochondria isolated from *Elovl3*-ablated mice (*M*), 2 µM FCCP, 30 µM palmitoyl-CoA. Medium contained 5 mM DL-carnitine.

Results in Fig. 3*C* and Table 1 show that the mitochondrial capacity of utilizing fatty acids for oxidation was not affected in *Elovl3*-ablated mice.

Increased Muscle Shivering in the Elovl3-ablated Mice—We have shown that, although the *Elovl3*-ablated mice showed normal mitochondrial capacity for oxidizing fatty acids, the mice were unable to hyperactivate their brown adipose tissue in order to maintain normal body temperature at 4 °C. To analyze whether the hyperinduced metabolic rate in the cold-acclimated *Elovl3*-ablated mice included an increased activity in other heat-producing sources, such as increased muscle activity (shivering), we performed electromyogram measurements. Since the skin of the *Elovl3*-ablated mice was very elastic and loose, the contact between muscle and electrode was weak, and as a result, the recorded signal was low as well. As a consequence, comparison of the absolute values obtained for the wild-type and *Elovl3*-ablated mice is not valid. Instead, the parameter of interest is the difference in magnitude of muscle electrical activity at 30 and 4 °C. In agreement with previous data (31), there was no major difference in muscle electrical activity of cold-acclimated wild-type mice and *Elovl3*-ablated mice kept at thermoneutrality (Fig. 4, *A* and *B*), demonstrating that these mice possessed satisfactory body temperature maintenance. However, there was a clear difference for the *Elovl3*-ablated mice, since muscle electrical activity was much higher at 4 °C than at 30 °C (Fig. 4*B*). This demonstrates that the hyperinduced metabolic rate in *Elovl3*-ablated mice was not due to a greater capacity of BAT for heat production but rather was the sum of adrenergically stimulated thermogenesis (nonshivering) and muscle-derived thermogenesis (shivering).

TABLE 1

Oxygen consumption in brown fat mitochondria from wild-type and *Elovl3*-ablated mice

The rates of oxygen consumption of brown fat mitochondria are expressed as nmol of O_2 min^{-1} mg $protein^{-1}$. Pyruvate was 5 mM, malate was 3 mM, and GDP was 2 mM. Maximal rate of oxygen consumption (state uncoupled) was induced by titration of FCCP (2.0–2.8 µM). 50 µM palmitoyl-L-carnitine or 30 µM palmitoyl CoA + 5 mM carnitine or 60 µM palmitate + 1 mM ATP + 5 mM carnitine + 20 µM CoA-SH were used for investigation of fatty acid oxidation. 2.0 µM FCCP was added to mitochondria in fatty acid oxidation analysis. The values are means ± S.E. of four independent mitochondria isolations for each group. Media composition and experimental conditions of isolation and analysis are described under "Experimental Procedures."

Process and rates of oxygen consumption	+/+ ($n = 4$)	−/− ($n = 4$)
UCP-dependent oxygen consumption and oxidative capacity		
Substrate (pyruvate + malate)	112.3 ± 3.3	110.4 ± 8.4
GDP	31.2 ± 3.4	29.1 ± 3.6
UCP1-dependent (substrate-GDP)	81.2 ± 0.8	81.4 ± 6.4
State uncoupled (FCCP)	170.2 ± 8.3	174.1 ± 15.9
Fatty acid oxidation		
Palmitoyl-L-carnitine	239.6 ± 19.1	223.5 ± 21.0
Palmitoyl-CoA (+carnitine)	229.9 ± 18.9	231.2 ± 21.7
Palmitate (+CoA-SH, +ATP, +carnitine)	155.7 ± 13.9	156.7 ± 10.9

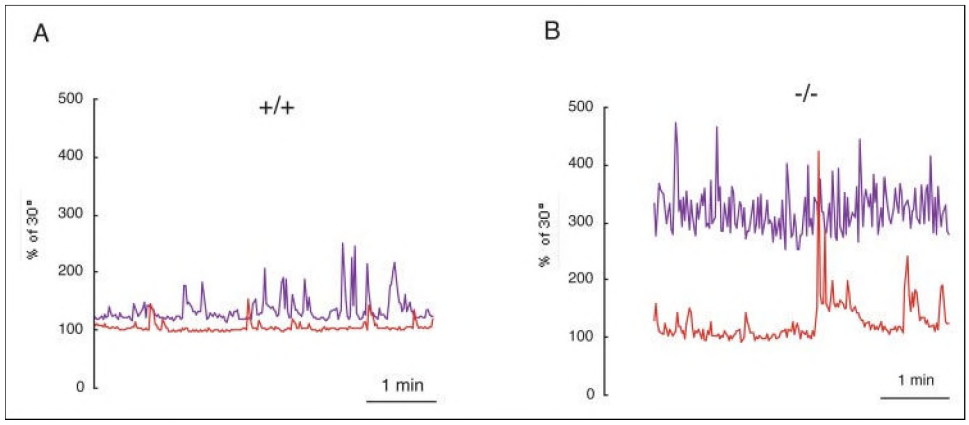

FIGURE 4. **Increased muscle shivering in cold-acclimated *Elovl3*-ablated mice.** Three-week cold-acclimated mice were placed in a chamber at 4 °C and muscle activity was recorded (*blue line*). The same mice were used for measurement of basal muscle activity at 30 °C (*red line*). Representative recordings from wild-type (+/+) (*A*) and *Elovl3*-ablated (−/−) (*B*) mice are shown.

Elovl3-ablated Mice Have a Temporally Diminished Ability to Elongate Fatty Acyl-CoAs—We have recently shown that *Elovl3*-ablated mice have an altered composition of saturated and monounsaturated VLCFA in their hair lipids (25), which is in agreement with the postulated function of ELOVL3 (15). Therefore, we performed experiments in order to elucidate a putative difference in the ability of brown adipose tissue to synthesize VLCFA in isolated microsomes from brown fat of wild-type and *Elovl3*-ablated mice after 3 days of cold stress (*i.e.* when the *Elovl3* mRNA level in wild-type mice was at a maximum), and at 3 weeks, when the mice were fully cold-acclimated.

Results in Fig. 5 show that the elongation activity in wild-type mice increases 6–10 times in cold compared with warm-acclimated mice when using palmitoyl-CoA (C16:0 CoA) as a substrate. These results were representative for stearoyl-CoA (C18:0 CoA) precursor as well (not shown). When we compared the elongation activity between wild-type and *Elovl3*-ablated mice, 3 days cold-exposed *Elovl3*-ablated mice demonstrated a significant decrease in elongation capacity compared with the control mice. With palmitoyl-CoA (C16:0 CoA) as substrate, the elongation activity was about 40% of control, whereas with arachidoyl-CoA (C20:0 CoA) as substrate, the elongation activity was further decreased to about 20% of that in control mice (Fig. 6*A*). Surprisingly, the difference in elongation capacity between wild-type and *Elovl3*-ablated mice was abolished in mice kept in the cold for 3 weeks (Fig. 6*B*).

Decreased Elongation Activity of the Condensation Step in the Elovl3-ablated Mouse—The four-step reaction cycle in the biosynthesis of VLCFAs is regulated by the first rate-limiting condensation step, since the activities of the proceeding (NADPH-dependent) reductases and dehydrase are 1–3 orders of magnitude greater than the condensing enzyme (19). This implies that the condensing enzyme controls fatty acid chain elongation. Regarding the importance of *Elovl3* for the condensation step, this hypothesis can be addressed by omitting NADPH from the microsomal reaction mixture. The reaction will then accumulate the condensation product β-ketoacyl-CoA and will not be able to proceed any further.

When we analyzed microsomes from 3-day cold-exposed mice in the absence of NADPH, the elongation decreased to 5–10% of the activity found in microsomes when NADPH was present in the solution. However, the relative difference in elongation activity between wild-type and *Elovl3*-ablated mice was always similar, irrespective of the presence or absence of NADPH (compare Fig. 6*A*). With palmitoyl-CoA (C16:0 CoA) as substrate, the activity was 60% of the control value (Fig. 7*A*), and with arachidoyl-CoA (C20:0 CoA) as substrate, the elongation activity was 15% of that in control microsomes (Fig. 7*B*), as was the relative decrease in total enzyme activity when NADPH was included (Fig. 6*A*).

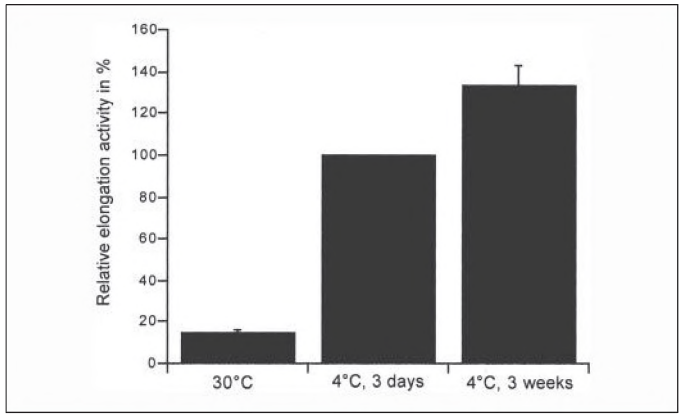

FIGURE 5. **Increased fatty acid elongation activity in brown fat microsomes from cold-exposed mice.** Relative elongation activity of palmitoyl-CoA (C16:0 CoA) in brown fat microsomes from wild-type mice exposed 3 days or 3 weeks to cold. Mice acclimated to 30 °C are included as controls. The values of 3-day cold-stressed (4 °C) mice are normalized to 100%. Each *bar* represents two or three independent experiments on microsomes pooled from seven mice in each. The values are expressed as means and with S.E. for 30 °C and 3-week cold-acclimated mice.

This confirms that ELOVL3 is controlling the rate-limiting condensation step in the elongation reaction.

Unaffected Expression of Elovl1 in Elovl3-ablated Mice—In mammals, fatty acids up to 16 carbons in length are generally synthesized by the cytosolic enzyme fatty acid synthase (FAS) (35). The resulting acyl chains can then be further elongated by elongases within the endoplasmic reticulum. Since ELOVL1 and ELOVL3 have been proposed to elongate saturated and monounsaturated fatty acids and to have overlapping activities, as seen by complementation studies in yeast (*i.e.* ELOVL1 is suggested to elongate VLCFAs of up to 26 carbon atoms, whereas ELOVL3 elongates VLCFAs of up to 24 carbon atoms (15)), we asked whether there was increased expression of *Elovl1* in the *Elovl3*-ablated mice, explaining a compensatory mechanism in 3-week cold-acclimated mice (*cf* Fig. 6*B*). As shown in Fig. 8, there was no statistical difference in mRNA levels between cold-exposed control and *Elovl3*-ablated mice at any time. This is in accordance with our earlier results showing no effect on *Elovl1* expression of cold exposure (15). In addition, there was no difference in *Fas* (fatty acid synthase) or *Acc* (acetyl CoA carboxylase) expression as well as of any polyunsaturated fatty acid elongase (*Elovl2*, *-4*, and *-5*) between cold-acclimated wild-type and *Elovl*-ablated mice (not shown).

Changes in Levels of Individual VLCFAs in Elovl3-ablated Mice—In order to see if the difference in microsomal elongation activity between *Elovl3*-ablated mice cold-stimulated 3 days and 3 weeks was paralleled by changes in specific VLCFA, we performed gas chromatography anal-

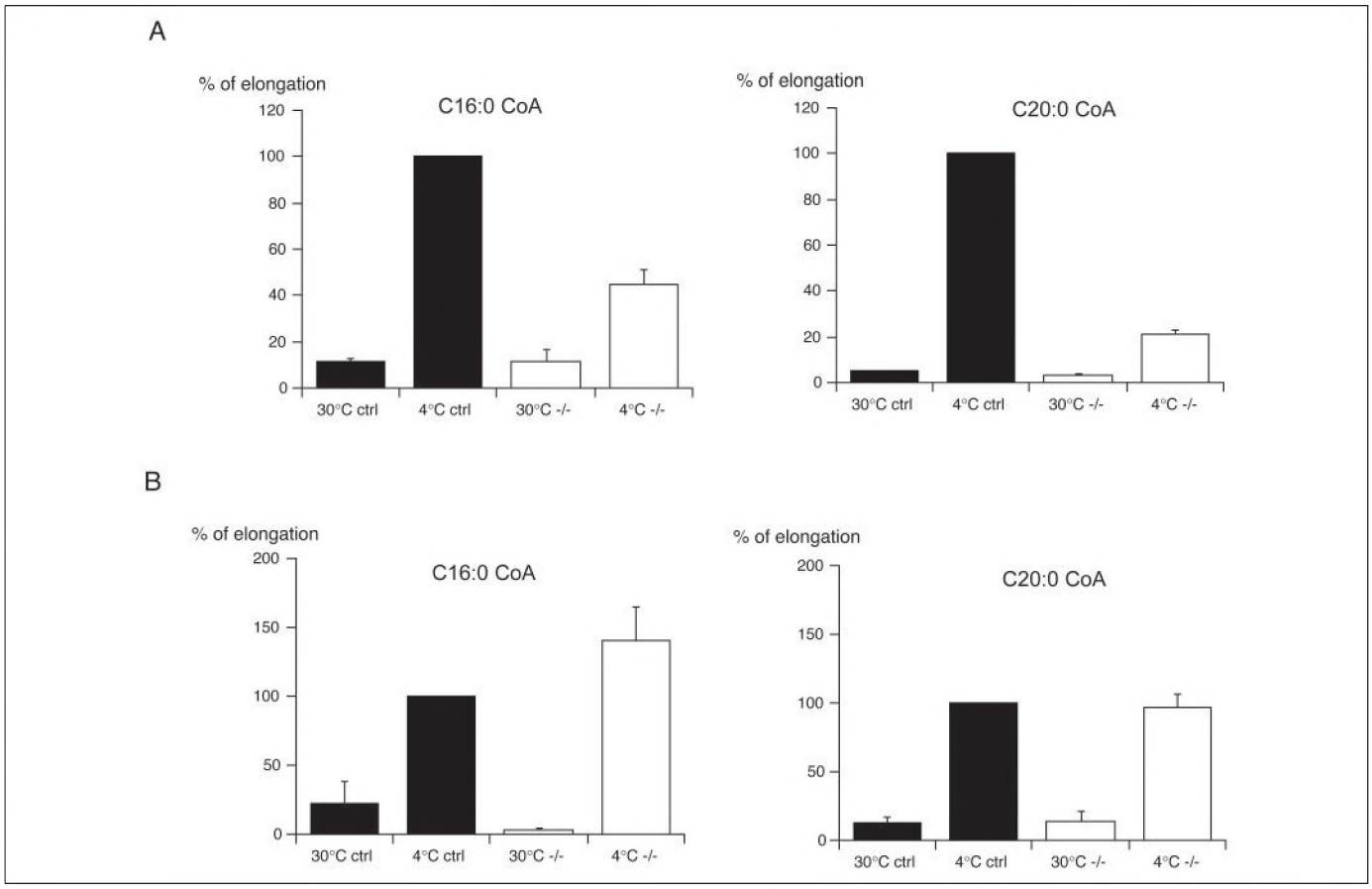

FIGURE 6. **Disturbed fatty acid elongation activity in cold-stressed *Elovl3*-ablated mice.** Elongation activity in brown fat microsomes is shown. Relative NADPH-supported elongation activity in microsomes from wild-type and *Elovl3*-ablated mice with palmitoyl-CoA (C16:0 CoA) and arachidoyl-CoA (C20:0 CoA) as substrate is shown. Microsomes from wild-type mice, exposed for 3 days (*A*) and 3 weeks (*B*) to 4 °C, were each normalized to 100%. Each *bar* represents the mean of 2–4 independent experiments with 6–8 animals pooled in each.

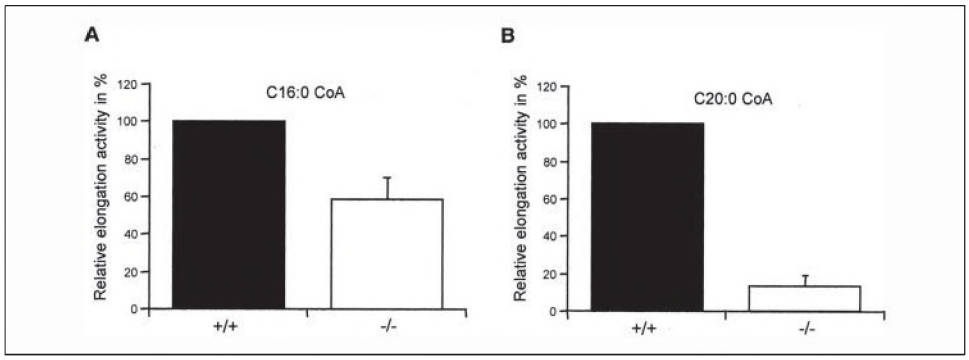

FIGURE 7. **Diminished activity of the condensation step of fatty acid elongation in brown fat microsomes from *Elovl3*-ablated mice.** Relative condensation activity in microsomes from 3-day cold-exposed (4 °C) wild-type and *Elovl3*-ablated mice, with palmitoyl-CoA (C16:0 CoA) (*A*) and arachidoyl-CoA (C20:0 CoA) (*B*) as substrates. Each *bar* represents two or three independent experiments with seven mice pooled in each with S.E. The control values are normalized to 100%.

ysis on extracted glycerolipids from brown adipose tissue. As seen in Table 2, although the amount of stearic acid (C18:0) was slightly less in control mice, it was approximately doubled in both the control and the *Elovl3*-ablated mice after 3 days of cold exposure. However, the levels of arachidic (C20:0) and behenic (C22:0) acid were suppressed in the *Elovl3*-ablated mice to the same extent as the elongation activity of C20:0 in the same animals (*i.e.* about 20% of normal levels) (Table 2, Fig. 6*A*). After 3 weeks in the cold, both wild-type and *Elovl3*-ablated mice had approximately similar amounts of C18:0 and C22:0, whereas C20:0 was only increased in *Elovl3*-ablated mice to about one-third of the level seen in control mice.

The results for the polyunsaturated fatty acids arachidonic acid (C20:4) and docosahexaenoic acid (C22:6) (Table 3) contrast with those for saturated fatty acids. The amount of arachidonic acid and docosahexaenoic acid was more increased in brown adipose tissue from 3-day cold-exposed *Elovl3*-ablated mice compared with control mice. In 3-week cold-acclimated mice, as with the saturated fatty acids, there were similar amounts of C20:4 and C22:6 in the brown adipose tissue from both types of mice. Eicosapentaenoic acid (C20:5) was increased in cold-acclimated mice in both strains (Table 3).

Since it is well documented that mice show increased food intake when exposed to cold, we analyzed whether the increase in certain polyunsaturated fatty acids in the *Elovl3*-ablated mice could be linked to a greater food intake in these mice. As seen in Table 4, food intake per kg of body weight was significantly increased in the knock-out mice already during the first week of cold exposure. After 3 weeks, the increase was

17% above that for control mice. Despite an elevated food intake, the *Elovl3*-ablated mice did not weigh more than the control mice. Instead, when we analyzed the total fat content in 4-weeks cold-exposed mice, the *Elovl3*-ablated mice contained less fat (17%) than control mice (22%). This shows that the increased energy expenditure in cold-exposed *Elovl3*-ablated mice could not be fully compensated by increased food intake.

Impaired Fat Accumulation and Metabolic Capacity in Warm-acclimated Elovl3-ablated Mice—Since *Elovl3*-ablation has been shown to cause hyperplastic sebocytes with a disturbed triglycerides content of saturated and monounsaturated VLCFA (25), we asked whether the disturbed content of VLCFA in the brown adipocytes had any effect on fat accumulation in these mice. In general terms, the recruitment process of brown adipose tissue is initiated when animals experience cold and the adrenergic pathway is activated. In nonactivated tissue, the mature cells fill up with fat droplets as energy reserves for combustion upon norepinephrine stimulation. This can be seen in wild-type mice when comparing Fig. 9*A* (+/+, 30 °C *versus* 4 °C). Unexpectedly, in 3-week warm-acclimated *Elovl3*-ablated mice, the brown adipose tissue seemed shrunken (not shown) and showed dramatically reduced fat droplets within the vast majority of the brown adipocytes (Fig. 9*A* (−/−, 30 °C)). After 3 days or 3 weeks of cold exposure, cells from both wild-type and *Elovl3*-ablated mice displayed similar phenotypes (*i.e.* many small fat droplets, which is consistent with activated brown fat tissue). This result suggests that even at 30 °C, the *Elovl3*-ablated mice are unable to accumulate fat.

Under normal conditions, *Elovl3* expression is not detectable in brown adipose tissue in warm-acclimated wild-type mice using Northern blot analysis. In order to ascertain whether any *Elovl3* expression really occurs within the tissue in 3-week warm-acclimated, "non-cold-stimulated," wild-type mice, reverse transcription-PCR analysis was performed. As seen in Fig. 9, *B* and *C*, a specific fragment of 381 bp, originating from *Elovl3* mRNA, was detected in wild-type mice. In *Elovl3*-ablated mice, only a 603-bp-long fragment, originating from distorted transcripts, was detected.

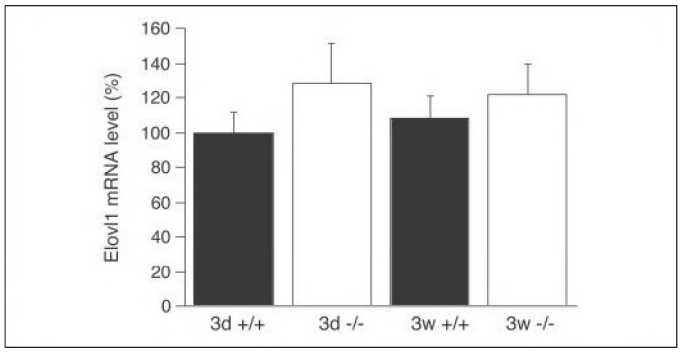

FIGURE 8. **Unaffected *Elovl1* mRNA levels in *Elovl3*-ablated mice.** Northern blot analysis of *Elovl1* mRNA expression from brown adipose tissue in wild-type and *Elovl3*-ablated mice exposed to 4 °C for 3 days or 3 weeks. Each *bar* represents the mean value of three independent experiments with three animals in each. Ten μg of total RNA was loaded into each lane.

TABLE 2

Levels of saturated fatty acids in brown adipose tissue

Levels of stearic acid (C18:0), arachidic acid (C20:0), and behenic acid (C22:0) in brown adipose tissue were determined by gas-chromatographic analysis from wild-type and *Elovl3*-ablated mice exposed to 30 °C for 10 days and to 4 °C for 3 days or 3 weeks. Each value is represented by a pool of three animals.

Fatty acid	Wild-type			*Elovl3*-ablated		
	30 °C	4 °C 3 days	4 °C 3 weeks	30 °C	4 °C 3 days	4 °C 3 weeks
18:0	6.1	10.4	16.4	8.5	16.7	16.3
20:0	0.3	0.5	0.6	0.1	<0.1	0.2
22:0	<0.1	0.4	0.3	<0.1	<0.1	0.3

TABLE 3

Levels of (*n*-6) and (*n*-3) polyunsaturated fatty acid in brown adipose tissue

Levels of PUFA belonging to the (*n*-6) and (*n*-3) family in brown adipose tissue were determined by gas-chromatographic analysis from wild-type and *Elovl3*-ablated mice exposed to 30 °C for 10 days and to 4 °C for 3 days or 3 weeks. Each value is represented by a pool of three animals.

	Wild type			*Elovl3*-ablated		
	30 °C	4 °C 3 days	4 °C 3 weeks	30 °C	4 °C 3 days	4 °C 3 weeks
(*n*-6)						
18:2	25.8	29.3	22.2	25.9	32.5	23.6
20:2	0.2	0.2	0.2	0.3	<0.1	0.2
20:3	0.1	0.1	0.3	0.1	0.3	0.2
20:4	0.4	1.0	6.2	0.6	3.1	5.4
(*n*-3)						
18:3	1.4	1.0	0.4	1.3	0.6	0.6
20:5	0.1	0.2	0.9	<0.1	<0.1	0.9
22:5	0.1	0.1	0.2	0.1	0.2	0.2
22:6	1.0	1.2	3.4	1.0	2.6	2.6

TABLE 4

Food intake and body weight in wild-type and *Elovl3*-ablated mice at 4 °C

Food intake and body weight were measured for wild-type and *Elovl3*-ablated mice housed at 4 °C at the indicated times. The values represent means ± S.E. based on 4 mice in each group. Statistical difference between wild-type and *Elovl3*-ablated mice is calculated with an unpaired *t*-test.

	0 days in cold	3 days in cold	7 days in cold	21 days in cold
Food intake				
Wild-type	0	21.4 ± 1.3	54.4 ± 2.3	184.8 ± 9.0
Elovl3-ablated	0	21.9 ± 1.9	59.2 ± 2.5	216.6 ± 17.3[a]
Body weight				
Wild-type	28.4 ± 0.8	NM[b]	29.2 ± 0.8	29.6 ± 0.8
Elovl3-ablated	26.8 ± 1.1	NM[b]	27.3 ± 1.4	29.7 ± 0.4

[a] $p < 0.05$.
[b] NM, not measured.

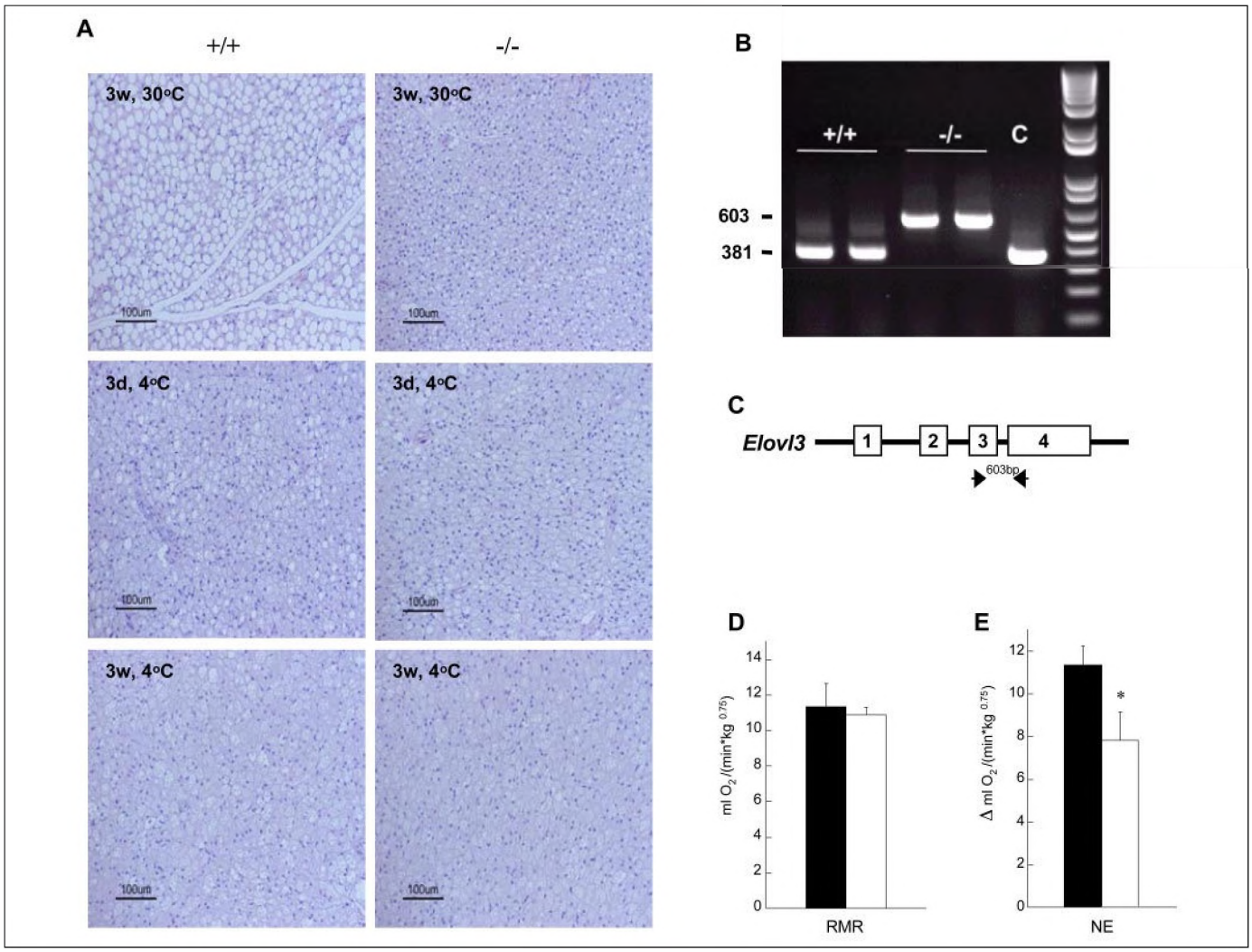

FIGURE 9. **Impaired fat accumulation and metabolic capacity in warm-acclimated Elovl3-ablated mice.** *A*, microscopic overview of interscapular brown adipose tissue from wild-type and *Elovl3*-ablated mice housed at 30 °C for 3 weeks or at 4 °C for 3 days or 3 weeks, respectively. *B*, DNase-treated total RNA (2.5 mg) was reverse-transcribed and amplified with *Elovl3*-specific primers. *Lanes 1* and *2*, wild-type mice; *lanes 3* and *4*, *Elovl3*-ablated mice; *lane 5*, cold-stimulated wild-type brown adipose tissue (0.25 mg). *M*, 1 kb Plus DNA Ladder molecular weight marker (Invitrogen). *C*, schematic overview of the *Elovl3* exon/intron structure and the sites of the PCR primers. *D*, resting metabolic rate (*RMR*) of 3-week warm-acclimated (30 °C) wild-type and *Elovl3*-ablated mice determined at 30 °C for 3 h. The values represent means ± S.E., based on 5 wild-type (*black bars*) and *Elovl3*-ablated (*white bars*) mice in each group. *E*, relative increase in metabolic rate after NE (1 mg/kg of body weight) injection of anesthetized 3-week warm-acclimated (30 °C) wild-type and *Elovl3*-ablated mice determined at 30 °C for 3 h. The values represent means ± S.E., based on seven wild-type mice (*black bars*) and six *Elovl3*-ablated mice (*open bars*) in each group. Statistical differences between wild-type and *Elovl3*-ablated mice are calculated with an unpaired *t* test. *, $p < 0.05$.

Since the most pronounced effect on fatty acid formation in *Elovl3*-ablated mice was detected at thermoneutrality and within the first days of cold exposure, we analyzed the metabolic capacity of the brown adipose tissue by injecting NE into warm-acclimated anesthetized mice at 30 °C.

As seen for cold-acclimated mice in Fig. 2*B*, no difference in oxygen consumption between warm-acclimated wild-type and *Elovl3*-ablated mice could be detected at 30 °C (Fig. 9*D*). When norepinephrine was injected, there was a low but significant increase in oxygen consumption in both wild-type and *Elovl3*-ablated mice. However, the relative increase (shown as Δ values) in *Elovl3*-ablated mice was significantly lower than for the wild-type mice, indicating that the metabolic capacity of the brown adipose tissue in these mice is reduced (Fig. 9*E*).

DISCUSSION

Although the existence of a machinery to elongate fatty acids from the FAS complex has been known for a long time, one exciting development over the last decade has been to identify the genes and proteins involved in the elongation pathways of fatty acids and their specific roles in lipid formation. In this paper, we present data that show that the elongase ELOVL3 does affect the condensation reaction, which is the rate-limiting step for the elongation cycle of VLCFAs (16–19).

All *Elovl* genes show a distinct tissue-specific expression pattern, and one intriguing question is why brown adipose tissue requires an increase in *Elovl3* mRNA levels of 2 orders of magnitude in cold-exposed mice. Surprisingly, the lack of *Elovl3* did not obviously impair the ability of brown adipose tissue to function as a heat-producing organ. However, even if the *Elovl3*-ablated mice experienced the cold more acutely than wild-type mice, due to an impaired skin barrier (25), the *Elovl3*-ablated mice were unable to hyperactivate their brown adipose tissue, as estimated by normal levels of *Ucp1* expression after cold stimulation and the inability of norepinephrine to hyperinduce oxygen consumption in these mice. Instead, they generated more heat by muscle shivering. Our previous study on the skin barrier of these mice showed that although the *Elovl3*-ablated mice could withstand a 4 °C cold exposure, as shown in this study, they were unable to maintain their body temperature with

wet fur (due to an impaired water repulsion) even at room temperature (22 °C) (25). Together with the present data on 3 weeks of cold acclimation, it suggests that the brown adipose tissue of *Elovl3*-ablated mice has a limited ability to develop and to produce heat and that the maximal value of activity has been reached in these mice.

The synthesis of VLCFAs was clearly affected in 3-day cold-stressed mice. Since the effect disappeared within 3 weeks of cold exposure, one can always speculate on a compensatory mechanism in the cold with time in the mutant mice. As described earlier (15, 36), the ability of *Elovl1* and *Elovl3* to complement each other in yeast mutants indicated a similar function for the two proteins (*i.e.* involvement in the synthesis of saturated and monounsaturated VLCFAs with 26 and 24 carbons, respectively). Analysis of the expression of *Elovl1* in the *Elovl3*-ablated mice failed to show any compensatory mechanism through *Elovl1* at the mRNA level. However, it is still possible that a compensation can occur on the level of protein activity, although it is difficult to imagine that the 100-fold induction of *Elovl3* expression could be compensated by a similar activity of the ELOVL1 protein without having effects on the level of other VLCFA species such as C26 fatty acids, which have been shown to be the major products of *Elovl1* activity. In addition, to date, there are no data available that suggest any regulatory mechanism other than the level of transcription in controlling the activity of the enzymes (including FAS) involved in fatty acid elongation. Since the phenotype of the *Elovl3*-ablated mice is clearly manifested in the skin, where *Elovl1* is also normally expressed (15, 25), no obvious compensatory mechanism for loss of *Elovl3* was developed there. Although the elongation activity is strongly decreased in microsomes of cold-stressed *Elovl3*-ablated mice, there is a residual elongation activity that is ELOVL3-independent.

Most data on fatty acid content in brown adipose tissue are based on analysis of triglycerides and glycerophospholipids because of their importance as energy reserves and constituents of the cellular membranes, respectively. Together with previous data on the hair lipids of *Elovl3*-ablated mice, where the triglyceride pool showed the most dramatic changes in VLCFA levels (25), we here demonstrate that ELOVL3 has a role in the regulation of the amount of certain saturated and monounsaturated VLCFAs for triglyceride formation also in brown adipose tissue. An explanation for the dramatic differences in effects of *Elovl3* ablation between brown adipose tissue and skin may be found in their different areas of function and usage of similar lipid molecules. The triglycerides in the sebum are mainly hydrolyzed for glycerol production and hydration of the stratum corneum (37), whereas in brown adipose tissue, the main function of the triglycerides is for storage of fatty acids for combustion.

Cold acclimation leads to a decrease in total triglyceride content and an increase in total cholesterol and phospholipid levels in both mouse and rat brown adipose tissue (38–40). The latter is mainly due to an increase in the amount of mitochondrial membranes (41). Although there is a decrease in triglyceride content, there is at the same time an increased triacylglycerol/fatty acid turnover in brown adipose tissue, which can be detected already during the first day of cold exposure (42, 43). It is suggested that the decrease in triacylglycerol content seen with norepinephrine is secondary to activation of fatty acid oxidation (44). The triglycerides comprise ~75% of the total lipids in the interscapular brown adipose tissue of mice and are mainly composed of unsaturated fats, with oleic (18:1) and linoleic (18:2) acids predominating. Of the saturated fatty acids, palmitic (C16:0) and stearic (C18:0) acids appear to be the most prevalent (41, 45, 46).

The predominant acyl chains in the phospholipid fraction are very similar to the triglyceride content (39, 47). Although the amount of saturated fatty acids is increased (saturation index is increased) in cold-acclimated rats and monounsaturated fatty acids are decreased in the same animals (48), it has been shown that the phospholipids become more unsaturated and the triglycerides become more saturated with prolonged cold exposure (40).

The principal differences between *Elovl3*-ablated and wild-type mice were the reduced levels of C20:0 and C22:0 in cold-stressed *Elovl3*-ablated mice. This did not drastically affect the saturation index in the *Elovl3*-ablated mice, since the amount of stearic acid (C18:0) was higher in these animals, compared with wild-type mice. No difference could be seen between the two strains at 30 °C, primarily because of VLCFA levels too low to be analyzed. Although the levels of arachidic acid (C20:0) and behenic acid (C22:0) are very low compared with the bulk lipids in brown adipose tissue, it is shown that long hydrophobic fatty acids are important components in the formation of triglycerides (49). A dramatic change in the fatty acid composition of triglycerides (*e.g.* in *Elovl3*-ablated mice during cold exposure) may therefore drastically influence their metabolic fate. Since *Elovl3* expression is correlated with increased β-oxidation, the function of *Elovl3* is probably to replenish intracellular pools of saturated VLCFA when the fatty acid turnover rate is high.

Regarding polyunsaturated fatty acids, such as arachidonic acid (C20:4) and docosahexaenoic acid (C22:6), our analysis made on cold-acclimated wild-type mice supports earlier data indicating that these fatty acids are found to be increased in cold-acclimated mice and rats (38, 39, 47). Surprisingly, in 3-day cold-exposed mice (*i.e.* cold stress *versus* cold acclimation), we found that *Elovl3*-ablated mice but not wild-type mice also showed increased levels of arachidonic acid (C20:4) and docosahexaenoic acid (C22:6). One explanation for this could be that the *Elovl3*-ablated mice experienced the cold more strongly than wild-type mice, which also was emphasized in the shivering experiment. This, in turn, increased their metabolic activity and also their food intake, leading to increased tissue levels of, for example, arachidonic acid (C20:4) and docosahexaenoic acid (C22:6) from the high dietary content of these fatty acids. However, since cold-exposed *Elovl3*-ablated mice showed less fat mass than control mice, increased food intake could not fully compensate for the elevated energy expenditure seen in these mice. The reason for this is unclear. One explanation could be that the mice are unable to eat more or that the capacity of food utilization has reached its maximum. Since regular chow diet contains limited amounts of calories, this may simply not be enough in a situation like this.

The fact that warm-acclimated *Elovl3*-ablated mice had dramatically reduced fat content in their brown adipocytes as well as diminished metabolic capacity, even when fed *ad libitum* with normal diet, underlines the importance of *Elovl3* in the control of lipid recruitment, even before any cold stimuli has been encountered. We have earlier shown that induced *Elovl3* expression in brown adipocytes is dependent on a combination of both norepinephrine and glucocorticoid exposure (14). Together with our data presented here, this suggests that there is a low, but significant, basal *Elovl3* activity of fatty acid elongation in brown adipose tissue in wild-type mice, which is controlled by serum factors (*e.g.* glucocorticoids). The activity can then be further stimulated by cold exposure via the adrenergic pathway as fatty acid oxidation is induced and, accordingly, an increased demand for fatty acid supplementation is required. This is in line with our recent data showing that induced lipolysis is required for optimal *Elovl3* expression in brown fat cells (51).

Finally, since differences in fatty acid composition, as well as in elongation activity, were detected only in cold-stressed mice, one can assume that an essential role for ELOVL3 activity in brown adipose

tissue could be found only during the early recruitment process of the tissue. However, since the *Elovl3*-ablated mice were unable to hyperinduce their brown adipose tissue after prolonged cold stimulation, it suggests that the optimal function of brown adipose tissue is reduced also in cold-acclimated *Elovl3*-ablated mice.

Acknowledgments—We thank Dr. C. Carneheim, B. Leksell, and B. Jungbjer for technical assistance and Jan Nedergaard and Barbara Cannon for valuable discussions.

REFERENCES

1. Jansky, L. (1973) *Biol. Rev.* **48,** 85–132
2. Foster, D. O., and Frydman, M. L. (1979) *Can. J. Physiol. Pharmacol.* **57,** 257–270
3. Enerbäck, S., Jacobsson, A., Simpson, E. M., Guerra, C., Yamashita, H., Harper, M.-E., and Kozak, L. P. (1997) *Nature* **387,** 90–94
4. Trayhurn, P. (1986) in *Brown Adipose Tissue* (Trayhurn, P. and Nichols, D. G., eds) pp. 299–338, Edward Arnold Ltd., London, UK
5. Jacobsson, A., Mühleisen, M., Cannon, B., and Nedergaard, J. (1994) *Am. J Physiol.* **267,** R999–R1007
6. Cannon, B., and Nedergaard, J. (2004) *Physiol. Rev.* **84,** 277–359
7. Trayhurn, P., and Ashwell, M. (1987) *Proc. Nutr. Soc.* **46,** 135–142
8. Cannon, B., Jacobsson, A., Rehnmark, S., and Nedergaard, J. (1996) *Int. J. Obes.* **20,** S36–S42
9. Cameron, I. L., and Smith, R. E. (1964) *J Cell Biol.* **23,** 89–100
10. Bukowiecki, L. J., Collet, A. J., Follea, N., Guay, G., and Jahjah, L. (1982) *Am. J. Physiol.* **242,** E353–E359
11. Géloën, A., Collet, A. J., Guay, G., and Bukowiecki, L. J. (1988) *Am. J. Physiol.* **254,** C175–C182
12. Rehnmark, S., and Nedergaard, J. (1989) *Exp. Cell Res.* **180,** 574–579
13. Jacobsson, A., Stadler, U., Glotzer, M. A., and Kozak, L. P. (1985) *J. Biol. Chem.* **260,** 16250–16254
14. Tvrdik, P., Asadi, A., Kozak, L. P., Nedergaard, J., Cannon, B., and Jacobsson, A. (1997) *J. Biol. Chem.* **272,** 31738–31746
15. Tvrdik, P., Westerberg, R., Silve, S., Asadi, A., Jakobsson, A., Cannon, B., Loison, G., and Jacobsson, A. (2000) *J. Cell Biol.* **149,** 707–717
16. Nugteren, D. H. (1965) *Biochim. Biophys. Acta* **106,** 280–290
17. Bernert, J. T., and Sprecher, H. (1977) *J. Biol. Chem.* **252,** 6736–6744
18. Bernert, J. T., Bourre, J. M., Baumann, N. A., and Sprecher, H. (1978) *J Neurochem.* **32,** 85–90
19. Suneja, S. K., Nagi, M. N., Cook, L., and Cinti, D. L. (1991) *J. Neurochem.* **57,** 140–146
20. Moon, Y. A., Shah, N. A., Mohapatra, S., Warrington, J. A., and Horton, J. D. (2001) *J. Biol. Chem.* **276,** 45358–45366
21. Leonard, A. E., Bobik, E. G., Dorado, J., Kroeger, P. E., Chuang, L.-T., Thurmond, J. M., Parker-Barnes, J. M., Das, T., Huang, Y.-S., and Mukerji, P. (2000) *Biochem. J.* **350,** 765–770
22. Inagaki, K., Aki, T., Fukuda, Y., Kawamoto, S., Shigeta, S., Ono, K., and Suzuki, O. (2002) *Biosci. Biotechnol. Biochem.* **66,** 613–621
23. Leonard, A. E., Kelder, B., Bobik, E. G., Chuang, L. T., Lewis, C. J., Kopchick, J. J., Mukerji, P., and Huang, Y. S. (2002) *Lipids* **37,** 733–740
24. Zhang, K., Kniazeva, M., Han, M., Li, W., Yu, Z., Yang, Z., Li, Y., Metzker, M. L., Allikmets, R., Zack, D. J., Kakuk, L. E., Lagali, P. S., Wong, P. W., MacDonald, I. M., Sieving, P. A., Figueroa, D. J., Austin, C. P., Gould, R. J., Ayyagari, R., and Petrukhin, K. (2001) *Nat. Genet.* **27,** 89–93
25. Westerberg, R., Tvrdik, P., Undén, A. B., Månsson, J. E., Norlén, L., Jakobsson, A., Holleran, W. M., Elias, P. M., Asadi, A., Flodby, P., Toftgård, R., Capecchi, M. R., and Jacobsson, A. (2004) *J. Biol. Chem.* **279,** 5621–5629
26. Dicker, A., Cannon, B., and Nedergaard, J. (1995) *Am. J. Physiol.* **269,** R767–R774
27. Cannon, B., and Nedergaard, J. (2001) *Methods Mol. Biol.* **155,** 295–303
28. Udenfriend, S., Stein, S., Bohlen, P., Dairman, W., Leimgruber, W., and Weigele, M. (1972) *Science* **178,** 871–872
29. Bradford, M. M. (1976) *Anal. Chem.* **72,** 248–254
30. Svennerholm, L., and Fredman, P. (1980) *Biochim. Biophys. Acta* **617,** 97–109
31. Golozoubova, V., Hohtola, E., Matthias, A., Jacobsson, A., Cannon, B., and Nedergaard, J. (2001) *FASEB J.* **15,** 2048–2050
32. Hohtola, E. (1982) *Comp. Biochem. Physiol.* **73A**, 159–166
33. Nedergaard, J., and Cannon, B. (1992) in *New Comprehensive Biochemistry*, Vol. 23 (Ernster, L., ed) pp. 385–420, Elsevier, Amsterdam, The Netherlands
34. Shabalina, I. G., Jacobsson, A., Cannon, B., and Nedergaard, J. (2004) *J. Biol. Chem.* **279,** 38236–38248
35. Smith, S. (1994) *FASEB J.* **8,** 1248–1259
36. Silve, S., Leplatois, P., Josse, A., Dupuy, P. H., Lanau, C., Kaghad, M., Dhers, C., Picard, C., Rahier, A., Taton, M., Le Fur, G., Caput, D., Ferrara, P., and Loison, G. (1996) *Mol. Cell. Biol.* **16,** 2719–2727
37. Fluhr, J. W., Mao-Qiang, M., Brown, B. E., Wertz, P. W., Crumrine, D., Sundberg, J. P., Feingold, K. R., and Elias, P. M. (2003) *J Invest. Dermatol.* **120,** 728–737
38. Senault, C., Hlusko, M. T., and Portet, R. (1975) *Ann. Nutr. Alim.* **29,** 67–77
39. Ricquier, D., Mory, G., and Hemon, P. (1979) *Can. J. Biochem.* **57,** 1262–1266
40. Ogawa, K., Ohno, T., and Kuroshima, A. (1992) *Jpn. J Physiol.* **42,** 63–73
41. Smith, R. E., and Horwitz, B. A. (1969) *Physiol. Rev.* **49,** 330–425
42. Lindberg, O., Bieber, L. L., and Houstek, J. (1976) in *Regulation of Depressed Metabolism and Thermogenesis* (Jansky, L., and Musacchia, X. J., eds) pp. 117–136, Thomas, Springfield, OH
43. Brooks, B. J., Arch, J. R., and Newsholme, E. A. (1983) *Biosci. Rep.* **3,** 263–267
44. Baht, H. S., and Saggerson, E. D. (1989) *Biochem. J.* **258,** 369–373
45. Bukowiecki, L. J., Follea, N., Lupien, J., and Paradis, A. (1981) *J. Biol. Chem.* **256,** 12840–12848
46. Carneheim, C. M. H., Cannon, B., and Nedergaard, J. (1989) *Am. J. Physiol.* **256,** R146–R154
47. Cannon, B., Polnaszek, C. F., Butler, K. W., Eriksson, L. E. G., and Smith, I. C. P. (1975) *Arch. Biochem. Biophys.* **167,** 505–518
48. Ogawa, K., Ohno, T., and Kuroshima, A. (1987) *Jpn. J. Physiol.* **37,** 783–796
49. Raclot, T. (2003) *Prog. Lipid Res.* **42,** 257–288
50. Alberts, P., Johansson, B. G., and McArthur, R. A. (2005) *Current Protocols in Pharmacology*, pp. 5.39.1–5.39.15, Suppl. 28, John Wiley & Sons, Inc., New York
51. Jakobsson, A., Jorgensen, J. A., and Jacobsson, A. (2005) *Am. J. Physiol.* **289,** E517–E526